

Figure 9. Diagram of the Michelson interferometer. A single ray of light is split into two rays by mirror M_0 , which is called a beam splitter. The path difference between the two rays is varied with the adjustable mirror M_1 . As M_1 is moved, an interference pattern changes in the field of view.

Circular fringes

These are produced with monochromatic light when the mirrors are in exact adjustment and are the ones used in most kinds of measurement with the interferometer. Their origin can be understood by reference to the diagram of Fig.10. Here the real mirror M_2 has been replaced by its virtual image M_2' formed by reflection in G_1 . M_2' is then parallel to M_1 . Owing to the several reflections in the real interferometer, we may now think of the extended source as being at L , behind the observer, and as forming two virtual images L_1 and L_2 in M_1 and M_2' . These virtual sources are coherent in that the phases of corresponding points in the two are exactly the same at all instants. If d is the separation $M_1 M_2'$, the virtual sources will be separated by $2d$. When d is exactly an integral number of

half wavelengths, i.e., the path difference $2d$ equal to an integral number of whole wavelengths, all rays of light reflected normal to the mirrors will

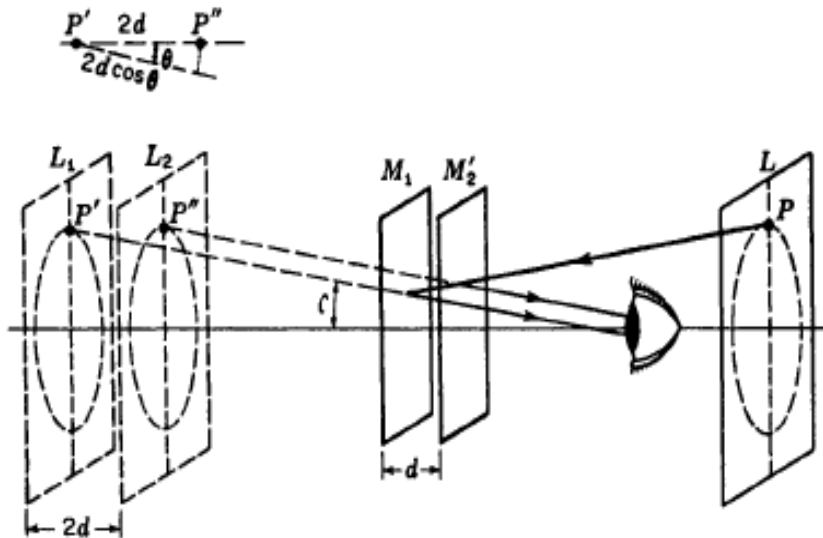


Figure 10 Formation of circular fringes in the Michelson interferometer.

be in phase. Rays of light reflected at an angle, however, will in general not be in phase. The path difference between the two rays coming to the eye from corresponding points P' and P'' is $2d\cos\theta$, as shown in the figure. The angle θ is necessarily the same for the two rays when M_1 is parallel to M_2' so that the rays are parallel. Hence when the eye is focused to receive parallel rays (a small telescope is more satisfactory here, especially for large values of d) the rays will reinforce each other to produce maxima for those angle θ satisfying the relation.

$$2d\cos\theta = m\lambda \quad (7)$$

Since for a given m , λ , and d the angle θ is constant, the maxima will lie in the form of circles about the foot of the perpendicular from the eye to the mirrors. By expanding the cosine, it can be shown from Eq.6 that the radii of the rings are proportional to the square roots of integers. The intensity distribution across the rings follows $I = A^2 = 4a^2 \cos^2 (\delta/2)$, in which the phase difference is given by

$$\delta = (2\pi/\lambda) 2d\cos\theta$$

Fringes of this kind, where parallel beams are brought to interference with a phase difference determined by the angle of inclination θ , are often referred to as fringes of equal inclination.

When M_1 at the position a few centimeters beyond M_2' , the fringe system will have the general appearance shown in (a) with the rings very closely spaced. If M_1 is now moved slowly toward M_2' so that d is decreased, Eq.7 shows that a given ring, characterized by a given value of the order m , must decrease its radius because the product $2d\cos\theta$ must remain constant. The rings therefore shrink and vanish at the center, a ring disappearing each time $2d$ decreases by λ , or d by $\lambda/2$. This follows from the fact that at the center $\cos\theta = 1$, so that Eq.6 becomes

$$2d = m\lambda \quad (8)$$

To change m by unity, d must change by $\lambda/2$. Now as M_1 approaches M_2' the rings become more widely spaced, as indicated in Fig.10A(b), until finally we reach a critical position where the central fringe has spread out to cover the whole field of view. This happens when M_1 and M_2' are exactly coincident, for it is clear that under these conditions the path difference is zero for all angles of incidence. If the mirror is moved still farther, it effectively passes through M_2' , and new widely spaced fringes appear, growing out from the center. These will gradually become more closely spaced as the path difference increases.

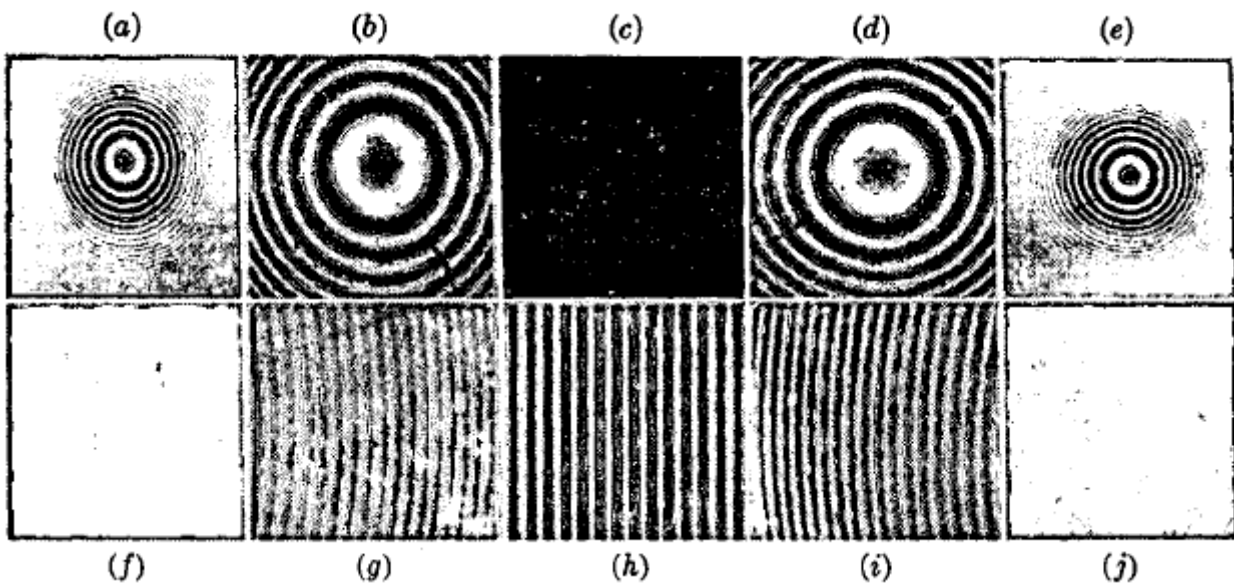


Fig.10A: Appearance of the various types of fringes observed in the Michelson interferometer.

Localized fringes

If the mirrors M_2' and M_1 are not exactly parallel, fringes will still be seen with monochromatic light for path difference not exceeding a few millimeters. In this case the space between the mirrors is wedge-shaped, as indicated in Fig11. The two rays reaching the eye from a point P on the source are now no longer parallel, but appear to diverge from a point P' near the mirrors.

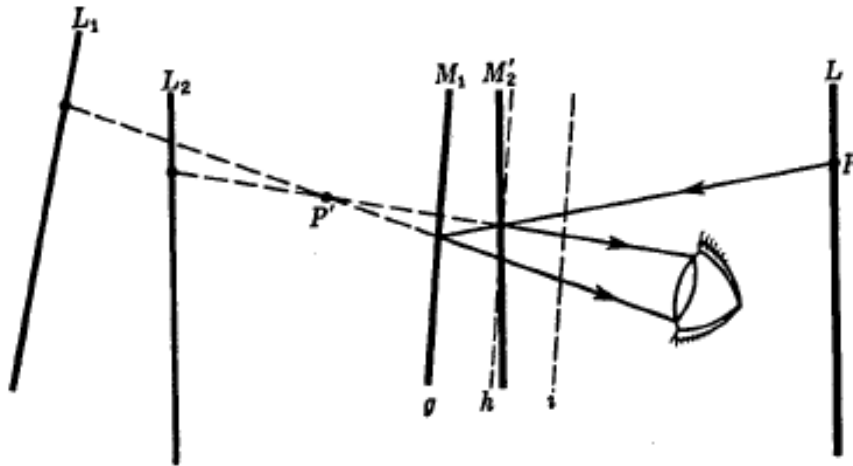


Fig.11 The formation of fringes with inclined mirrors in the Michelson interferometer.

For various positions of P on the extended source, it can be shown that the path difference between the two rays remains constant but that the distance of P' from the mirrors changes. If the angle between the mirrors is not too small, however, the latter distance is never great, and hence, in order to see these fringes clearly, the eye must be focused on or near the rear mirror M_1 . The localized fringes are practically straight because the variation of the path difference across the field of view is now due primarily to the variation of the thickness of the 'air film' between the mirrors. With a wedge-shaped film, the locus of points of equal thickness is a straight line parallel to the edge of the wedge. The fringes are not exactly straight, however, if d has an appreciable value, because there is also some variation of the path difference with angle. They are in general curved and are always convex toward the thin edge of the wedge.

White-light fringes

If a source of white light is used, no fringes will be seen at all except for a path difference so small that it does not exceed a few wavelengths. In observing these fringes, the mirrors are tilted slightly as for localized fringes, and the position of M_1 is found where it intersects M_2' . With white light there will then be observed a central dark fringe, bordered on either side by 8 or 10 colored fringes. This position is often rather troublesome to find using white light only. It is best located approximately

beforehand by finding the place where the localized fringes in monochromatic light become straight. Then a very slow motion of M_1 through this region, using white light, will bring these fringes into view.

The fact that only a few fringes are observed with white light is easily accounted for when we remember that such light contains all wavelengths between 400 and 750 nm. The fringes for a given color are more widely spaced the greater the wavelength. Thus the fringes of different colors will only coincide for $d=0$, as indicated in Fig 12. The solid curve represents the intensity distribution in the fringes for green light, and the broken curve that for red light.

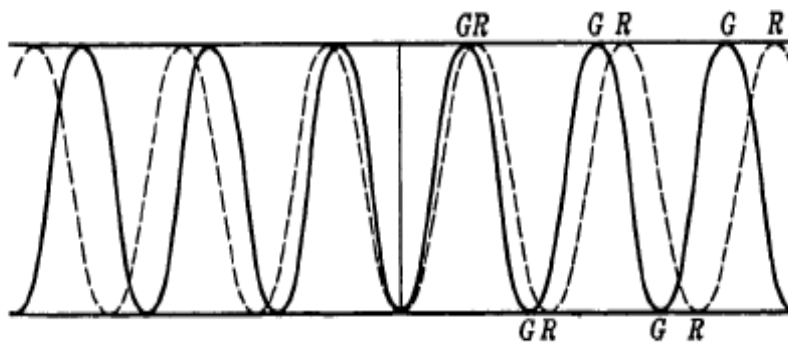


Figure 12 The formation of white-light fringes with a dark fringe at the center.

Visibility of the fringes

There are three principal types of measurement that can be made with the interferometer: (1) width and fine structure of spectrum lines, (2) lengths or displacements in terms of wavelengths of light, and (3) refractive indices. S explained in the preceding section, when a certain spread of wavelengths is present in the light source, the fringes become indistinct and eventually disappear as the path difference is increased.

Michelson tested the lines from various sources and concluded that a certain red line in the spectrum of cadmium was the most satisfactory. He measured the visibility, defined as

$$V = \frac{I_{\max} - I_{\min}}{I_{\max} + I_{\min}} \quad (9)$$

Where I_{\max} and I_{\min} are the intensities at maxima and minima of the fringe pattern.

The more slowly V decreases with increasing path difference.

It is found that with sodium light the fringes become alternately sharp and diffuse, as the fringes from the two D lines get in and out of step. The number of fringes between two successive positions of maximum visibility is about 1000.

An alternative way of interpreting the eventual vanishing of interference at large path differences is instructive to consider at this point. It was indicated that a finite

spread of wavelengths corresponds to wave packets of limited length, this length decreasing as the spread becomes greater. Thus, when the two beams in the interferometer traverse distances that differ by more than the length of the individual packets, these can no longer overlap and no interference is possible. The situation upon complete disappearance of the fringes is shown schematically in Fig.13. The original wave packet P has its amplitude divided at G_1 so that two similar packets are produced, P_1 traveling to M_1 and P_2 to M_2 . When the beams are reunited, P_2 lags a distance $2d$ behind P_1 . Evidently a measurement of this limiting path difference gives a direct determination of the length of the wave packets.

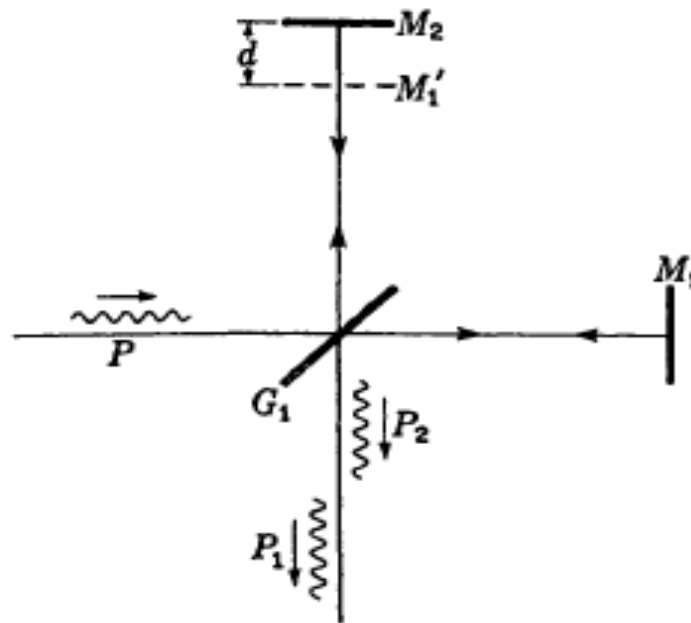


Fig.13 Limiting path difference as determined by the length of wave packets.

Interferometric measurements of length

When the mirror M_1 of Fig.9 is moved slowly from one position to another, counting the number of fringes in monochromatic light which cross the center of the field of view will give a measure of the distance the mirror has in terms of λ , since by Eq.10

$$2d = m\lambda$$

We have, for the position d_1 corresponding to the bright fringe of order m_1 ,

$$2d_1 = m_1\lambda$$

and for d_2 , giving a bright fringe of order m_2 , $2d_2 = m_2\lambda$

Subtracting these two equations, we find

$$d_1 - d_2 = (m_1 - m_2)\lambda/2 \quad \dots\dots\dots (10)$$